



**HAL**  
open science

## Comparative study of two atomic layer etching processes for GaN

Cédric Mannequin, Christophe Vallée, Katsuhiko Akimoto, Thierry Chevolleau, Christophe Durand, Christian Dussarrat, Takashi Teramoto, Etienne Gheeraert, Henri Mariette

► **To cite this version:**

Cédric Mannequin, Christophe Vallée, Katsuhiko Akimoto, Thierry Chevolleau, Christophe Durand, et al.. Comparative study of two atomic layer etching processes for GaN. *Journal of Vacuum Science & Technology A*, 2020, 38 (3), pp.032602. 10.1116/1.5134130 . hal-02917577

**HAL Id: hal-02917577**

**<https://hal.univ-grenoble-alpes.fr/hal-02917577v1>**

Submitted on 22 Sep 2021

**HAL** is a multi-disciplinary open access archive for the deposit and dissemination of scientific research documents, whether they are published or not. The documents may come from teaching and research institutions in France or abroad, or from public or private research centers.

L'archive ouverte pluridisciplinaire **HAL**, est destinée au dépôt et à la diffusion de documents scientifiques de niveau recherche, publiés ou non, émanant des établissements d'enseignement et de recherche français ou étrangers, des laboratoires publics ou privés.

# Comparative study of two atomic layer etching processes for GaN

Cite as: J. Vac. Sci. Technol. A **38**, 032602 (2020); <https://doi.org/10.1116/1.5134130>

Submitted: 30 October 2019 . Accepted: 03 March 2020 . Published Online: 26 March 2020

Cédric Mannequin, Christophe Vallée, Katsuhiko Akimoto, Thierry Chevolleau, Christophe Durand, Christian Dussarrat, Takashi Teramoto,  Etienne Gheeraert, Henri Mariette, et al.

## COLLECTIONS

Paper published as part of the special topic on [Special Topic Collection on Atomic Layer Etching \(ALE\)](#)

 This paper was selected as Featured



View Online



Export Citation



CrossMark

## ARTICLES YOU MAY BE INTERESTED IN

[Overview of atomic layer etching in the semiconductor industry](#)

Journal of Vacuum Science & Technology A **33**, 020802 (2015); <https://doi.org/10.1116/1.4913379>

[Selective atomic layer etching of HfO<sub>2</sub> over silicon by precursor and substrate-dependent selective deposition](#)

Journal of Vacuum Science & Technology A **38**, 032601 (2020); <https://doi.org/10.1116/1.5143247>

[Inside the mysterious world of plasma: A process engineer's perspective](#)

Journal of Vacuum Science & Technology A **38**, 031004 (2020); <https://doi.org/10.1116/1.5141863>



Advance your science and  
career as a member of

**AVS**

LEARN MORE



# Comparative study of two atomic layer etching processes for GaN

Cite as: J. Vac. Sci. Technol. A **38**, 032602 (2020); doi: [10.1116/1.5134130](https://doi.org/10.1116/1.5134130)

Submitted: 30 October 2019 · Accepted: 3 March 2020 ·

Published Online: 26 March 2020



View Online



Export Citation



CrossMark

Cédric Mannequin,<sup>1,a)</sup> Christophe Vallée,<sup>1,2</sup> Katsuhiko Akimoto,<sup>1</sup> Thierry Chevolleau,<sup>2</sup> Christophe Durand,<sup>3</sup> Christian Dussarrat,<sup>4</sup> Takashi Teramoto,<sup>4</sup> Etienne Cheeraert,<sup>1,5</sup>  and Henri Mariette<sup>1,3,5</sup>

## AFFILIATIONS

<sup>1</sup>Institute of Applied Physics, Faculty of Pure and Applied Sciences, University of Tsukuba, Tsukuba 305-8573, Japan

<sup>2</sup>CNRS/LTM, University of Grenoble-Alpes, Grenoble 38000, France

<sup>3</sup>CEA/IRIG/PHELIQS, University of Grenoble-Alpes, Grenoble 38054, France

<sup>4</sup>Air Liquide Laboratories, Yokosuka 239-0847, Japan

<sup>5</sup>CNRS/Institut Néel, University of Grenoble-Alpes, Grenoble 38042, France

**Note:** This paper is part of the 2020 Special Topic Collection on Atomic Layer Etching (ALE).

<sup>a)</sup>**Electronic mail:** [mannequin.cedric.ga@u.tsukuba.ac.jp](mailto:mannequin.cedric.ga@u.tsukuba.ac.jp)

## ABSTRACT

Atomic layer etching (ALE) of Ga-polar GaN (0001) using a standard inductively coupled plasma-reactive ion etching system is achieved in this work. The sequential process is using Cl<sub>2</sub> to modify the surface in the adsorption step. For the activation step, the authors compare two rare gas plasmas, namely, Ar and Kr, and show a much larger and well-defined ALE window for the latter. The ALE of GaN is demonstrated by etching mesa structures masked with a photoresist. A constant etching rate per cycle of two monolayers is obtained. The experimental conditions of this self-limited process are found by changing both the adsorption and activation times, together with the source power. This provides an atomic-scale process for nanofabrication, with significant improvements to the GaN surface.

Published under license by AVS. <https://doi.org/10.1116/1.5134130>

## I. INTRODUCTION

One of the greatest characteristics of gallium nitride (GaN) and its related alloys with In and/or Al for applications in high-power microelectronic devices, such as power light emitting diode and high electron mobility transistors, is their strong bonding energies<sup>1,2</sup> of 11.5, 8.9, and 7.7 eV/bond for AlN, GaN, and InN, respectively. However, this chemical stability is a critical issue when dealing with the dry etching process of these nitride devices because it requires high ionic flux at high energies. Such plasma etching induces a lot of surface damage that is detrimental to the device performances; see the progress review by Eriguchi.<sup>3</sup> For example, the damage induced during the fabrication process of a recessed gate for an AlGaIn/GaN field effect transistor could drastically reduce the gate breakdown voltage.<sup>4</sup> Similarly, when dealing with optoelectronic devices, point defects induced by the etching can act as Shockley–Read–Hall nonradiative centers for the carriers<sup>5</sup> and/or as surface charged traps, which leads to Fermi-level pinning.<sup>6</sup> Moreover, by using a (0001) surface, the formation of a

nonstoichiometric surface appears due to preferential etching loss of one of the elements Ga or N.<sup>7</sup>

To overcome all these problems, atomic layer etching (ALE) processes are developed nowadays. ALE is a sequential and cyclic process, allowing, in principle, an atomically controlled layer-by-layer and selective etching of a targeted material. The ALE basic concept is to split the etch process into at least two separate steps: first modifying the surface and second removing the thin modified layer;<sup>8</sup> see Fig. 1(a). Moreover, ALE relies on the fact that both these steps, named hereafter adsorption and activation, respectively, are self-limited. The adsorption step amounts to controlled surface modification ideally to one monolayer (ML),<sup>9</sup> while the activation step relies on a controlled reaction to remove the upmost modified layer by thermal reaction, ionic bombardment, or photon irradiation. Then, the ALE process offers a more precise control by isolating steps in time and switching between the steps in a repeatable cycle, together with a less ion-induced damage. ALE is under development nowadays to achieve atomic-scale control for nanoscale

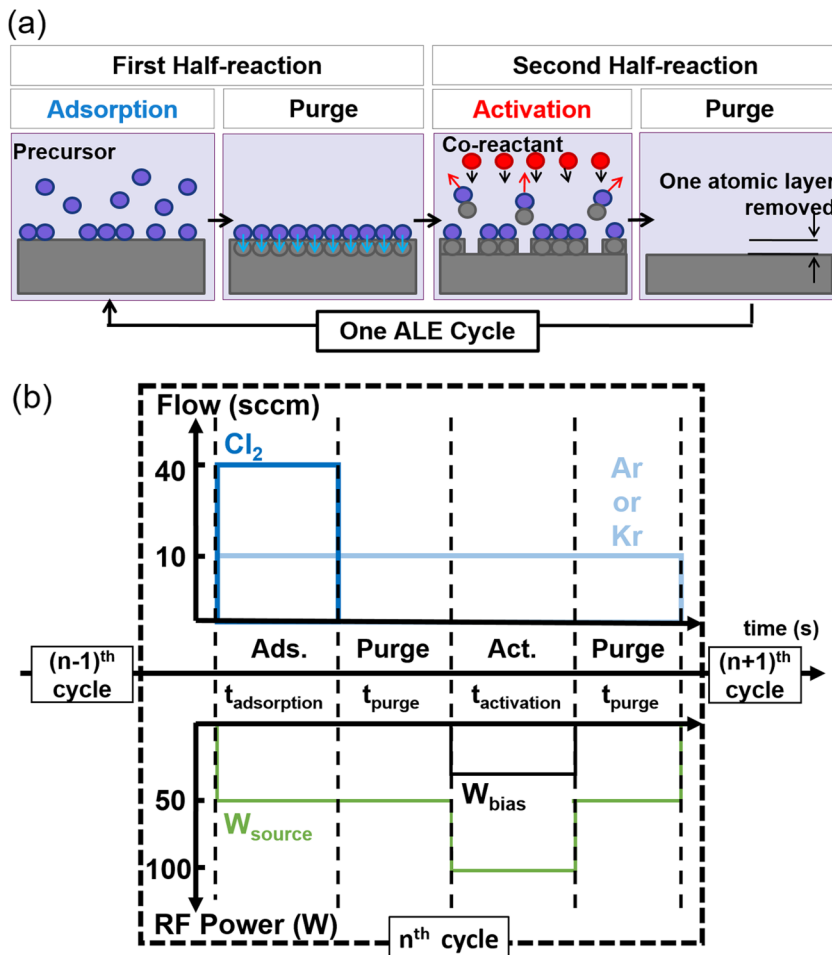


**FIG. 1.** Schematic representation of the two ALE half reactions: adsorption and activation (a). Schematic representation of one ALE cycle used in this study (b): a gas mixture consisting of Cl<sub>2</sub> and Ar or Kr at 40 and 10 SCCM, respectively, is used for the adsorption step. A constant flow of rare gas at 10 SCCM (Ar or Kr) is permanently maintained for the purge and activation step. RF<sub>source</sub> is maintained at 50 W for the adsorption step and the purge step and is increased to 100 or 120 W during the activation step. RF<sub>bias</sub> is only applied during the activation step in the 15–50 W range.

device fabrication for various materials including semiconductors, metals, and dielectrics; see the paper by Kanarik *et al.*<sup>10</sup>

For GaN, the reported plasma assisted ALE relies—regarding the adsorption step—either on oxidation, using O<sub>2</sub> plasma<sup>11,12</sup> or H<sub>2</sub>O<sub>2</sub> solution,<sup>13</sup> or on chlorination of GaN surfaces to form GaCl<sub>x</sub> by-products.<sup>14,15</sup> For the activation step, the use of Ar ion bombardment enables a unidirectional reaction, which is required for patterned features.<sup>14,15</sup>

In this work, we propose a comparative study of ALE processes for undoped, *c*-oriented, Ga-polar GaN, relying both on Cl<sub>2</sub> based plasma for the adsorption step, but which are using two different rare gases for the activation step, namely, Ar and Kr. Indeed, while most of the literature is devoted to the optimization of the ALE process, thanks to discussions about the adsorption step and the choice of the chemistry for this step, less work has been done on the understanding of the role of the rare gas, which is generally argon. Two recent papers have begun to look into the phenomena. First, Sherpa *et al.* have shown that in the ALE of Si by Cl<sub>2</sub>/Ar plasma,<sup>16</sup> the argon ions not only activate the modified SiCl<sub>x</sub> surface, which is crucial for the ALE window, but they also activate and create new Cl<sub>x</sub> adsorption sites (but no Si sputtering), which

can increase the Cl<sub>2</sub> saturation at the following adsorption steps. This surface modification by ion bombardment from 2D to “3D,” porosity, or roughness can also be at the origin of the observed drift in the ALE process yield between the very first cycle and the others. Second, Berry *et al.* have discussed a plasma ALE process based on the idea that only the sputtering of a thin modified layer occurs without damaging the underneath unmodified film.<sup>17</sup> Using a Monte Carlo collision cascade model, they predicted that depending on the rare gas used, a wider ALE window can be obtained for the ALE of tungsten. With this work, we will experimentally study this prediction for the ALE of GaN by comparing the use of two rare gas plasmas, namely, Ar and Kr.

## II. EXPERIMENT

Two ALE processes were developed in an inductively coupled plasma-reactive ion etching (ICP-RIE) etcher: RIE-200iP from SAMCO. *In situ* optical emission spectroscopy (OES) was used to monitor gas dissociation for the adsorption, activation, and purge steps, allowing the identification of active species. Additionally, OES monitoring was used to calibrate Cl<sub>2</sub> dosing

time and purging time to ensure complete separation of the  $\text{Cl}_2$  dissociation by-products and the gas used for the activation steps. The ICP source power ( $\text{RF}_{\text{source}}$ ) and pressure for the adsorption step were varied in the 5–120 W range at 0.65 Pa, respectively. For set adsorption step conditions, the DC self-bias ( $V_{\text{DC}}$ ) of the activation step was varied in the range of  $-11$  to  $-40$  V by changing the ICP bias power ( $\text{RF}_{\text{bias}}$ ); see the supplementary material<sup>31</sup> for tables presenting the measured  $|V_{\text{DC}}|$  corresponding to the  $\text{RF}_{\text{bias}}$  input. This assistance of substrate polarization in an ICP etcher ensures control of ion energy and enables activation through soft ionic bombardment calibrated to only sputter the modified layer. An Si wafer is introduced in the ICP reactor before conditioning the reactor chamber walls by an Ar/ $\text{Cl}_2$  plasma at the same  $\text{RF}_{\text{source}}$  and  $\text{RF}_{\text{bias}}$  conditions used for the adsorption step for 1 min. The reactor is then purged by  $\text{N}_2$ . During conditioning and ALE processing, the ICP reactor chamber walls are kept at  $150^\circ\text{C}$ . The chuck is maintained at a temperature of  $25^\circ\text{C}$  by water circulation. Temperature homogenization to the Si wafer is ensured by a helium backside cooling.

For each condition, the etching rate per cycle (EPC) was estimated from the depth of etched GaN submitted to 200 ALE cycles using scanning electron microscopy images and reported as a function of  $V_{\text{DC}}$  (from the activation step).

The specificity of our process is illustrated in Fig. 1(b): As far as the gases are concerned, pure rare gases (Ar and Kr) from Air Liquide were used. These gases were introduced in a continuous way, i.e., during all the steps including purge and activation steps. Considering  $\text{RF}_{\text{source}}$ , it is maintained at 50 W during adsorption and purge steps and increased in the 100–120 W range for the activation step, whereas  $\text{RF}_{\text{bias}}$  is only applied during the activation step. The advantage of this procedure is the possibility (i) to develop an ALE etching process in a conventional ICP etcher (no need of pulsed injection), (ii) to continuously monitor the ALE steps by OES, and (iii) to switch from conventional etching to ALE in the same process.

The samples consist of a  $3\ \mu\text{m}$  undoped *c*-axis oriented GaN epilayer grown on a sapphire substrate by metal organic chemical vapor deposition. An  $\text{SiO}_2$  hardmask was deposited by sputtering and patterned by photolithography into an array of  $3\ \mu\text{m}$ -diameter holes with  $2\ \mu\text{m}$  spacing. GaN/sapphire substrates were consecutively cleaned with acetone and then ethanol in an ultrasonic bath for 10 min. Each GaN sample was then patched on a 150 mm

diameter Si carrier wafer to be transferred. Before ALE processing, a soft sputtering of the GaN surface by Ar or Kr ions is performed for 30 s, in order to remove any GaN native oxide.

### III. RESULTS AND DISCUSSION

#### A. Ar versus Kr rare gas plasma

Figure 2 shows the results obtained for the EPC using exactly the same experimental conditions for all the ALE processing steps ( $\text{Cl}_2$  plasma with a pressure of 0.65 Pa), except the used rare gas, which was either Ar [Fig. 2(a)] or Kr [Fig. 2(b)]. Two features are revealed with the data presented in Figs. 2(a) and 2(b): (i) a clear plateau appears for the EPC when using Kr but not with Ar and (ii) a small increase in the EPC is observed for both activation gases, Ar and Kr, when increasing  $\text{RF}_{\text{source}}$  during the activation step.

The first result clearly shows a  $V_{\text{DC}}$  window, in the case of an activation step with Kr gas, for which a constant EPC is observed and is close to 0.52 nm/cycle. This value is in good agreement with the lattice constant of the GaN wurtzite crystal in the *c*-direction ( $5.189\ \text{\AA}$ ), which corresponds to two MLs of GaN. This regime was observed for  $V_{\text{DC}}$  in the range of  $[-16\ \text{V}, -22\ \text{V}]$ ; see Fig. 2(b). For energies below the lower limit of the  $V_{\text{DC}}$  window ( $-16\ \text{V}$ ), no measurable etched depth was observed from SEM images, hence the 0 nm/cycle attributed for these  $V_{\text{DC}}$  values. For energies above the upper limit ( $-22\ \text{V}$ ), the EPC linearly increased with the increase in  $V_{\text{DC}}$ .

By contrast, for Ar gas, the presence of a similar regime is not clear at all; only a narrow range of  $V_{\text{DC}}$   $[-15\ \text{V}, -17\ \text{V}]$  shows a smaller variation of EPC, around 0.4 nm/cycle, which corresponds to about 1.5 ML of GaN. For  $V_{\text{DC}}$  values above  $-17\ \text{V}$ , the EPC was found to increase, indicating an exit from the tenuous self-limited etching mode.

When increasing  $\text{RF}_{\text{source}}$  from 100 to 120 W, a small increase of EPC is observed even on the constant EPC regime, for both Ar and Kr gases. This second result indicates an effect of the ion density on the overall EPC, as also observed by Sherpa *et al.*<sup>16</sup> for the ALE of silicon with chlorine plasma.

#### B. Self-limited steps

Knowing that only Kr gas plasma gives rise to a clear constant EPC regime for a wide  $V_{\text{DC}}$  window, we concentrated our study on

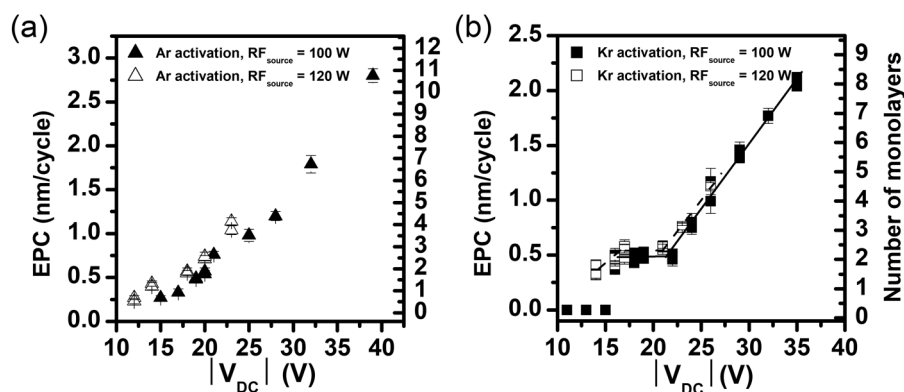
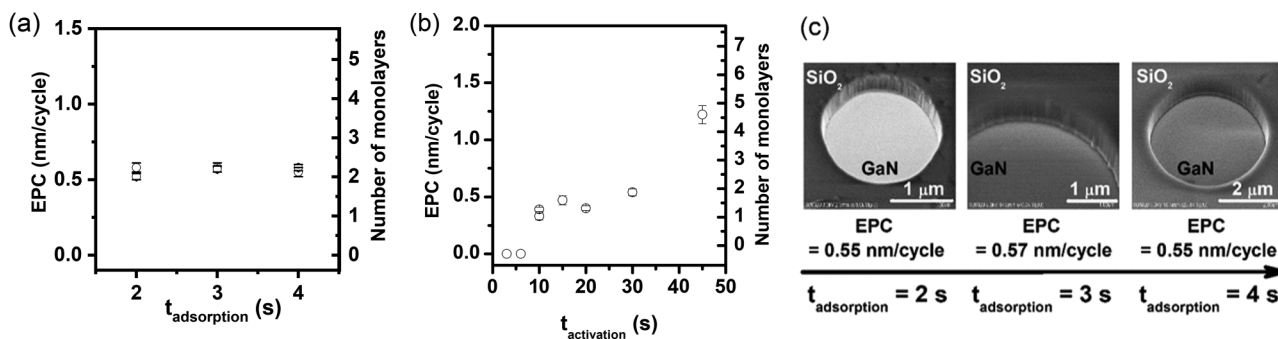


FIG. 2. EPC as a function of the absolute value of the self-bias potential  $V_{\text{DC}}$  by varying  $\text{RF}_{\text{bias}}$  for (a) an activation by Ar plasma with an  $\text{RF}_{\text{source}}$  set at 100 W (full triangle) and 120 W (empty triangle) and (b) an activation by Kr plasma for an  $\text{RF}_{\text{source}}$  set at 100 W (full square) and 120 W (empty square).



**FIG. 3.** EPC as a function of the adsorption time  $t_{\text{adsorption}}$  (a) and the activation time  $t_{\text{activation}}$  (b) for an in-window  $\text{Cl}_2/\text{Kr}$  ALE condition as reported in Fig. 2(b); gas flows,  $\text{RF}_{\text{source}}$ ,  $\text{RF}_{\text{bias}}$ , and other time parameters are kept constant. SEM images of GaN surfaces (c) with a  $\text{SiO}_2$  hardmask corresponding to the adsorption time  $t_{\text{adsorption}}$  investigated in (a).

the determination of self-limited behaviors for the adsorption and activation steps of our process, only for this rare gas. Figure 3 shows the stability of the EPC after changing the adsorption time  $t_{\text{adsorption}}$  [Figs. 3(a) and 3(c)] with a constant  $\text{RF}_{\text{source}}$  set at 50 W. For these experiments, the parameters of the activation steps were exactly the same. The EPC is constant over the studied parameter range, showing no additional impact on the EPC of the exposure time to the  $\text{Cl}_2/\text{Kr}$  plasma.

As far as the activation step is concerned, the activation time  $t_{\text{activation}}$  was varied over a large range of values from 5 to 50 s, keeping all the other parameters constant; see Fig. 4. A wide time window presenting a constant EPC is observed for exposure times between 10 and 30 s with an EPC value around 0.5 nm, in accordance with the EPC values obtained in Fig. 2(b). By contrast, for  $t_{\text{activation}}$  above 30 s, the EPC increased, indicating one or more additional phenomena for the etching mechanism.

### C. ALE synergy

A quantitative way to scale the degree to which a process approaches the ideal ALE regime is the “ALE synergy” parameter  $S$  as defined by Kanarik *et al.*<sup>10</sup> in Eq. (1),

$$\text{ALE synergy\% (S)} = \frac{\text{EPC} - (\alpha + \beta)}{\text{EPC}} \times 100\%. \quad (1)$$

EPC represents the material removed in one ALE cycle, averaging on either 200 completed ALE cycles or 400 cycles for the activation step. The values of  $\alpha$  and  $\beta$  are parasite etching contributions from individual steps, either adsorption or activation, when they are performed as independent processes. Ideally, synergy should approach 100% with no etching from either step alone. Figure 4(b) shows the results for the present case:  $\alpha = 0$ , corresponding to no background etching detected with exposure to  $\text{Cl}_2$  plasma only;  $\beta = 0.20$  nm/cycle, revealing that some sputtering of the Kr gas directly occurs on GaN materials. Having a value of EPC of 0.53 nm/cycle for ALE (full cycle), our synergy parameter is 62%. This value is below the one expected knowing that the GaN has a strong surface binding energy, which is favorable to achieve a well-controlled ALE process (see Ref. 10). It is also less than the

value of the synergy parameter  $S$  (0.90) reported by Ohba *et al.*<sup>14</sup> who had, nevertheless, a self-limited EPC in the ALE regime, which is not as well fixed, compared to the one reported herein.

### D. Surface morphology

From atomic force microscopy (AFM) observations, a significant decrease in the RMS roughness is obtained, from 0.18 nm for the as-deposited GaN surface to 0.07 nm after ALE processing. This smoothness is attributed to the layer-by-layer self-limiting nature of ALE as evidenced by contrast with the one obtained out of the ALE window (0.43 nm).

### E. Discussion

For activation by both Ar and Kr ions, the observed plateaus for the EPC at 0.4 and 0.52 nm/cycle, respectively, illustrate the concept of the ALE window as defined by Kanarik *et al.*<sup>9</sup> It allows

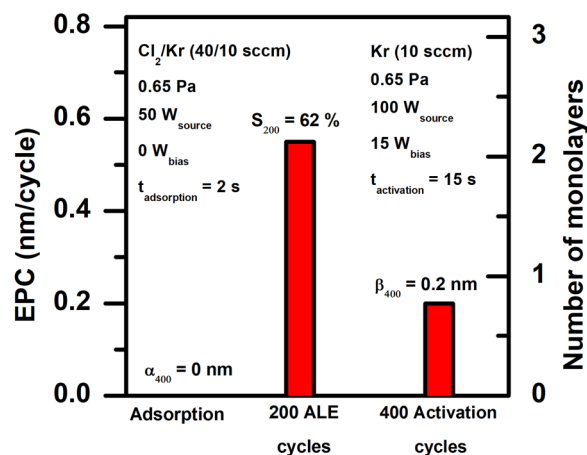


**FIG. 4.** Results of the  $\text{Cl}_2/\text{Kr}$  ALE synergy test. EPC after exposure to adsorption only and activation only for 400 cycles. In the middle bar, adsorption and activation are combined at the same conditions into an ALE for 400 cycles.

identification of an ALE window for a range of ion energies equivalent to  $V_{DC}$  windows of  $[-16\text{ V}, -22\text{ V}]$  and  $[-15\text{ V}, -17\text{ V}]$ , respectively, for Kr and Ar ions, for which the modified surface material assumed to be formed at the adsorption step is completely removed during the activation step. For Ar activation, the EPC at the ALE window is in good agreement with values in the 0.37–0.42 nm/cycle reported in the literature for ALE of GaN with Ar ion activation.<sup>14,15</sup> For energies below the lower limit of the ALE window,  $-16\text{ V}$  and  $-15\text{ V}$ , respectively, removal of the modified layer is assumed to be nonexistent or incomplete due to insufficient energy for the incoming ions. For energies above the upper limit,  $-22\text{ V}$  and  $-17\text{ V}$ , respectively, sputtering of bulk materials occurs without any self-limitation once the removal of the modified layer is completed. Sputtering thresholds in pristine Ga-polar GaN (0001) have been reported to be close to 100 eV and in the 250–400 eV range,<sup>18</sup> for N atoms and Ga atoms, respectively. The  $V_{DC}$  values reported here are not incompatible: the upper value reported for Ar ion activation is in good agreement with a  $V_{DC}$  of  $-16\text{ V}$  reported for the ALE of GaN with Ar activation in an ICP etcher reported by Kauppinen *et al.*<sup>15</sup>

The presence of a modified GaN layer at the end of the adsorption step is evidenced by the ALE synergy data presented in Fig. 4 and a lower EPC of 0.20 nm/cycle for the Kr adsorption step alone. These results also exclude direct Kr sputtering as an origin for the 0.52 nm/cycle at the ALE window, shown in Fig. 2(b). The nature of the modified layer formed at the surface of Ga-polar GaN (0001) has not yet been clearly experimentally identified. It is currently speculated to involve the adsorption of chlorine radicals and neutrals diffusing from the plasma to the Ga-polar surface<sup>14,19</sup> and/or the direct physisorption of nondissociated  $\text{Cl}_2$ ,<sup>15</sup> leading to the desorption of volatile by-products upon ionic bombardment at the activation step:  $\text{GaCl}_3$ ,<sup>14</sup>  $\text{GaCl}_2$ ,<sup>15</sup>  $\text{GaCl}$ ,  $\text{GaNCl}$ , and  $\text{Ga}_2\text{NCl}_2$ .<sup>19</sup> The underlying N dangling bonds are expected to recombine into  $\text{N}_2$  due to favorable high binding energy rather than from an N-rich surface.<sup>20</sup> The constant EPC as a function of  $t_{\text{adsorption}}$  presented in Fig. 3(a) confirms a clear self-limited saturation of available adsorption sites by chlorine species at the surface, as no increase of EPC occurs when increasing  $t_{\text{adsorption}}$  for identical Kr activation steps (same  $\text{RF}_{\text{source}}$  and  $\text{RF}_{\text{bias}}$  conditions).

We try to explain the difference in width for the observed ALE window between Ar and Kr ion gases, following the approach developed by Berry *et al.*<sup>17</sup> In their sputtering model, if you have a conserved momentum transfer, the sputtering yield should be ion mass dependent, especially for high atomic mass materials. They simulate that, for light material (titanium), the ion mass in the removal step does not change the ALE curve, whereas for the heavier one (tungsten), it is better to use a light rare gas such as neon instead of argon. Our experimental results confirm qualitatively the strong dependence of the ALE regime with the ion mass of the removal species, but not with the tendency predicted by Berry *et al.*,<sup>17</sup> i.e., the lighter the ion mass the larger the ALE window. In addition, the narrower ALE window for Ar ions could also originate from the difference in the ion energy distribution between Ar and Kr ions. The ion energy distribution for Ar plasma has been reported to be often wider than the ALE window.<sup>9,15</sup>

Kawakami *et al.*<sup>21</sup> reported a comparison of the GaN etching damage with both Kr and Ar plasma by using a capacitively coupled

radio frequency plasma generator. Kr plasma allows obtaining a smoother surface, a thinner etching depth, and a preferential etching of Ga species compared with Ar plasma, which leads to a preferential etching of N species and significant roughness of the GaN etched surface. The discrepancy observed between the difference in EPC at the ALE window between Kr ions (equivalent to two MLs of GaN) and Ar ions (equivalent to 1.5 ML of GaN) presented in this study and the thinner etch depth for Kr ions compared with Ar ions reported by Kawakami *et al.*<sup>21</sup> is still not clear. Two origins can be considered: (i) a partial removal of two modified MLs of GaN formed at the end of the adsorption step by Ar ions, compared with a full removal by Kr ions, or (ii) an overetch of one ML of GaN by Kr ions after removal of a single chlorinated GaN ML at the end of the adsorption, induced by the preferential etching of Ga atoms of the second ML. If we consider the case of adsorption of chlorine atoms for the formation of the modified layer, the optimal distance between chlorine atoms has been calculated to be greater than or equal to 0.36 nm.<sup>22</sup> The distance between two neighboring Ga atoms on a (0001) GaN surface is 0.319 nm. The mismatch is expected to lead to steric hindrances between Cl atoms impeding the full coverage of the surface and leaving nonpaired Ga atoms. Coverage of the Si surface by chlorine atoms has been reported in the 30%–50% range<sup>23,24</sup> and has been estimated to reach a maximum of 50% for the ALE of silicon.<sup>16,25</sup> Similar coverage is to be expected for the Ga-polar surface, excluding the first hypothesis. By assumption, a partial chlorination of only one ML of GaN, a preferential etching of the nonpaired Ga atoms by Kr ions compared with Ar ions could explain a difference in EPC, but it should yield at best, in the case of a self-limited activation, to an EPC of one ML and inferior to one ML for Kr and Ar ions, respectively. However, the preferential etching of Ga species by Kr ions could explain the especially low RMS roughness of 0.07 nm, reported in Fig. 5(e). By contrast, the higher propensity of Ar sputtering for damage introduction and the lack of assistance for removing nonpaired Ga atoms could explain the significantly higher RMS roughness at 1.9 nm reported for Ar activation based ALE of GaN.<sup>15</sup> The overetch per cycle of 1 and 0.4 ML for activation by Kr ions and Ar ions, respectively, could originate in a too-high  $\text{RF}_{\text{source}}$  and/or  $\text{RF}_{\text{bias}}$  used for the activation step: as a consequence, the synergetic effect<sup>26</sup> of neutral (chlorine radicals) and Kr ion bombardment during the adsorption and activation steps, respectively, is not completely separated in the process. This contrasts with the molecular dynamics simulation carried out on chemical sputtering of Cl-adsorbed wurzite GaN (0001) surfaces by Ar ions:<sup>19</sup> Ga is mainly sputtered in the form of  $\text{Ga-Cl}_2$ , but Ga sputtering does not take place at all on the clean surface for  $\text{RF}_{\text{source}}$  as large as 250 W. Finally, the presence of partially oxidized GaN at the surface originating from cross-contamination by oxygen desorbing from the  $\text{SiO}_2$  hardmask could lead to a difference in EPC if we consider a lower sputtering rate from Ar ions compared to Kr ions. The amount of desorbed oxygen is expected to be limited and not allow a full coverage of the GaN surface, as no degradation of the  $\text{SiO}_2$  hardmask was observed. However, only *in situ* XPS measurements would allow us to definitely exclude this possibility. While one of the hypotheses presented here could be contributing to the higher EPC at the ALE window observed for activation by Kr ions, nevertheless, additional mechanisms may contribute also.

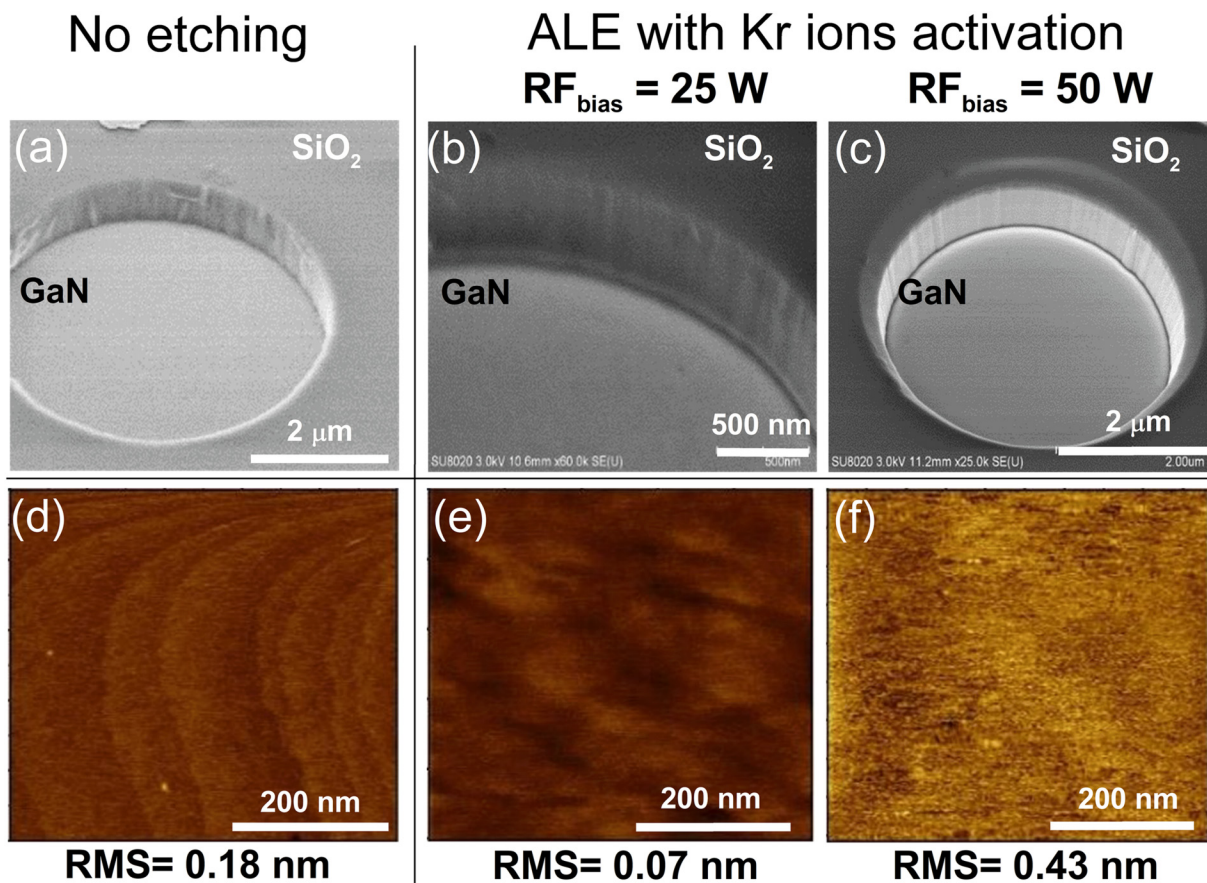


**FIG. 5.** SEM images of GaN surfaces with an SiO<sub>2</sub> hardmask: before etching (a) and after 200 cycles of the Cl<sub>2</sub>/Kr ALE process in the ALE window (b) and out of the ALE window (c). AFM images and RMS roughness of GaN surfaces: before etching (d) and after 200 cycles of the Cl<sub>2</sub>/Kr ALE process in the ALE window (e) and out of the ALE window (f).

Considering the small increase in EPC, even on the ALE plateau, when increasing the RF<sub>source</sub> for both Ar and Kr gases, similar EPC variations were reported by Sherpa *et al.*<sup>16</sup> for the ALE of silicon with chlorine plasma in a capacitively coupled plasma etcher. The authors associated this trend with an increase in adsorption sites during the ALE process. The increase in the ion density and ion flux, by increasing RF<sub>source</sub> from 100 to 120 W, leads to the creation at the *n*th activation step of additional adsorption sites for chlorine species at the following (*n* + 1)th adsorption step. The mechanisms for the creation of these additional active sites are still unclear, but the following mechanisms have been proposed for silicon by Sherpa *et al.*:<sup>16</sup> desorption of contaminants,<sup>27</sup> reductions in steric hindrances<sup>25</sup> between adsorbed chlorine species due to lattice deformations,<sup>24,28</sup> or creation of subsurface binding sites<sup>29</sup> upon ionic bombardment. This effect could be cumulative from the repetition of the activation step: as a consequence, the EPC reported in this study, averaged on 200 cycles, is not fully indicative to the instant etch depth at a given *n*th cycle.

In regard to the above discussion, the difference in EPC obtained at the ALE window between the two ion gases could be explained from the difference in the additional adsorption site

density introduced by the ionic bombardment for Ar and Kr ions. Such differences could arise from the difference in the ion mass, as mentioned earlier. It could be further widened by the higher ion fluxes obtained for Kr plasma compared with Ar plasma for the same RF<sub>source</sub> condition, originating from the lower ionization energy required for Kr (13.96 eV) compared with Ar (15.75 eV).<sup>21</sup>

The drift of EPC from an average of 0.5 to 1.18 nm/cycle for *t*<sub>activation</sub> above 30 s, shown in Fig. 3(b), illustrates a dose effect for the ionic bombardment impacting the EPC yield. High disordering and weakening of the GaN lattice induced by long exposure to soft ionic bombardment is assumed to either reduce the binding energy below the 8.6–9.12 eV range reported for the pristine GaN (0001) range<sup>1,14,21</sup> and reduce the threshold energy required for ions to sputter or drastically increase the density of adsorption sites at the GaN surface. In addition, the too-high value obtained for EPC when dealing only with Kr sputtering (Fig. 4) could then be explained by the dose effect mentioned above: we average here the EPC over 400 cycles and not 200 as for the completed ALE cycles, leading to an overestimated EPC.

These results reveal the nonideal achievement of the ALE condition for Kr ions: indeed, ion bombardment during the activation step, besides removing the modified layer, may also generate additional active sites for the adsorption of chlorine species. In other words, these results reveal that the usual assumption in ALE, that is, the steps of adsorption and desorption are fully decoupled, is not totally valid here and that more intricate relations between these two steps are at play.

#### IV. SUMMARY AND CONCLUSIONS

ALE of Ga-polar GaN (0001) using a standard ICP-RIE system is achieved in this work. We have investigated the use of two rare gas plasmas for the activation step, namely, Ar and Kr, and show a much larger and well-defined ALE window for the latter, always using chlorine for the adsorption step. The GaN ALE process is demonstrated by etching mesa structures masked with a photoresist. A self-limited etching rate per cycle of two monolayers is obtained. This provides an atomic-scale process for nanofabrication, knowing in addition that the smoothness of the structure is increased.

Further work is needed to understand the limitation of the synergy parameter and to identify the species in the modified layer after the adsorption step by doing some XPS measurements. Moreover, a comparison of the two polar GaN (0001) surfaces, Ga and N, will be done to elucidate the influence of surface structures (Ga or N dangling bonds<sup>30</sup>) on the achievement of a well-controlled ALE regime.

#### ACKNOWLEDGMENTS

The authors devote this article to the memory of C. You who was working with them on this subject for her Ph.D. thesis as a student of both the University of Grenoble-Alpes and the University of Tsukuba who suddenly passed away. This work was achieved in the frame of a joint research and educational program between the University of Tsukuba and Université Grenoble-Alpes. The authors would like to thank Masahiro Sasaki from the University of Tsukuba for his support and advice on this work. This study was supported by the Laboratoire d'Excellence LANEF in Grenoble (No. ANR-10-LABX-51-01).

#### REFERENCES

<sup>1</sup>A. David, B. Moran, K. McGroddy, E. Matioli, E. L. Hu, S. P. DenBaars, S. Nakamura, and C. Weisbuch, *Appl. Phys. Lett.* **92**, 113514 (2008).  
<sup>2</sup>W. Harrison, *Electronic Structure and the Properties of Solids* (Dover, New York, 1989).  
<sup>3</sup>K. Eriguchi, *Jpn. J. Appl. Phys.* **56**, 06HA01 (2017).

<sup>4</sup>C. H. Chen, S. Keller, E. D. Haberer, L. Zhang, S. P. Denbaars, E. L. Hy, and Y. Wu, *J. Vac. Sci. Technol. B* **17**, 2755 (1999).  
<sup>5</sup>W. Shockley and W. T. Read, Jr., *Phys. Rev.* **87**, 835 (1952).  
<sup>6</sup>R. Calarco, M. Marso, T. Richter, A. I. Aykanat, R. Meijers, A. V. D. Hart, T. Stoica, and H. Lüth, *Nano Lett.* **5**, 981 (2005).  
<sup>7</sup>K. J. Choi, H. W. Jang, and J. L. Lee, *Appl. Phys. Lett.* **82**, 1233 (2003).  
<sup>8</sup>T. Faraz, F. Roozbeem, H. C. M. Knoops, and W. M. M. Kessels, *ECS J. Solid State Sci. Technol.* **4**, 5023 (2015).  
<sup>9</sup>K. J. Kanarik, T. Lill, E. A. Hudson, S. Sriraman, S. Tan, J. Marks, V. Vahedi, and R. A. Gottscho, *J. Vac. Sci. Technol. A* **33**, 020802 (2015).  
<sup>10</sup>K. J. Kanarik *et al.*, *J. Vac. Sci. Technol. A* **35**, 05C302 (2017).  
<sup>11</sup>D. Buttari, S. Heikman, S. Keller, and U.K. Mishra, *Proceedings of the IEEE Lester Eastman Conference on High Performances Devices*, Newark, DE, 8 August 2002 (IEEE, New York, 2002), p. 461.  
<sup>12</sup>S. D. Burnham, K. Boutros, P. Hashimoto, C. Butler, D. W. S. Wong, M. Hu, and M. Micovic, *Phys. Status Solidi C* **7**, 2010 (2010).  
<sup>13</sup>D. H. van Dorp, S. Arnauts, F. Holsteyns, and S. De Gendt, *ECS J. Solid State Sci. Technol.* **4**, N5061 (2015).  
<sup>14</sup>T. Ohba, W. Yang, S. Tan, K. J. Kanarik, and K. Nojiri, *Jpn. J. Appl. Phys.* **56**, 06HB06 (2017).  
<sup>15</sup>C. Kauppinen, S. A. Khan, J. Sundqvist, D. B. Suyatin, S. Suihkonen, E. I. Kauppinen, and M. Sopanen, *J. Vac. Sci. Technol. A* **35**, 060603 (2017).  
<sup>16</sup>S. D. Sherpa, P. L. G. Ventzek, M. Lee, G. S. Hwang, and A. Ranjan, *J. Vac. Sci. Technol. A* **36**, 031303-1 (2018).  
<sup>17</sup>I. L. Berry, K. J. Kanarik, T. Lill, S. Tan, V. Vahedi, and R. A. Gottscho, *J. Vac. Sci. Technol. A* **36**, 01B105 (2018).  
<sup>18</sup>K. Harafuji and K. Kawamura, *Jpn. J. Appl. Phys.* **47**, 1536 (2008).  
<sup>19</sup>K. Harafuji and K. Kawamura, *Jpn. J. Appl. Phys.* **49**, 08JE03 (2010).  
<sup>20</sup>J. Sellés *et al.*, *Appl. Phys. Lett.* **109**, 231101 (2016).  
<sup>21</sup>R. Kawakami, T. Inaoka, K. Tominaga, and T. Mukai, *Jpn. J. Appl. Phys.* **48**, 08HF01 (2009).  
<sup>22</sup>S. Rivillon, Y. J. Chabal, L. J. Webb, D. J. Michalak, N. S. Lewis, M. D. Halls, and K. Raghavachari, *J. Vac. Sci. Technol. A* **23**, 1100 (2005).  
<sup>23</sup>T. Matsuura, J. Murota, Y. Sawada, and T. Ohmi, *Appl. Phys. Lett.* **63**, 2803 (1993).  
<sup>24</sup>S. D. Athavale and D. J. Economou, *J. Vac. Sci. Technol. B* **14**, 3702 (1996).  
<sup>25</sup>G. Kresse and J. Furthmüller, *VASP: The Guide* (Vienna University of Technology, Vienna, 2001).  
<sup>26</sup>J. W. Coburn and H. F. Winters, *J. Appl. Phys.* **50**, 3189 (1979).  
<sup>27</sup>A. Ranjan, M. Wang, S. D. Sherpa, V. Rastogi, A. Koshiishi, and P. L. G. Ventzek, *J. Vac. Sci. Technol. A* **34**, 31304 (2016).  
<sup>28</sup>N. C. M. Fuller, D. A. Telesca, V. M. Donnelly, and I. P. Herman, *Appl. Phys. Lett.* **82**, 4663 (2003).  
<sup>29</sup>N. Layadi, V. M. Donnelly, and J. T. C. Lee, *J. Appl. Phys.* **81**, 6738 (1998).  
<sup>30</sup>M. Hasegawa, T. Tsutsumi, A. Tanide, H. Kondo, K. Ishikawa, M. Sekine, and M. Hori, "In situ surface analysis of Ga dangling sites and chlorination layers for determining atomic layer etching properties of GaN," presented at 12th Asian-European International Conference on Plasma Surface Engineering, Jeju Island, Korea, 1-5 September 2019 (unpublished).  
<sup>31</sup>See supplementary material at <https://doi.org/10.1116/1.5134130> for tables of measured DC self-bias and ICP bias power input.